

Field Effects on the Refractive Index and Absorption Coefficient in AlGaAs Quantum Well Structures and Their Feasibility for Electrooptic Device Applications

YASUO KAN, HIDEO NAGAI, MASAMICHI YAMANISHI, MEMBER, IEEE, AND IKUO SUEMUNE

Abstract—Electroreflectance and electroabsorption measurements have been carried out to clarify field effects on the refractive index and absorption coefficient in AlGaAs quantum well structures. The observed electroreflectance spectra show very clear exciton-induced features at room temperature. A maximum variation of the refractive index in each quantum well at a photon energy near the lowest excitonic transition gap is obtained to be 4 percent induced by a 10^5 V/cm field modulation. Electroreflectance and electroabsorption spectra are shown to demonstrate a relation between dispersion curves of the field-induced variations in the refractive index and absorption coefficient in the quantum well structure. Based on the obtained results, operation of an electroabsorption modulator with the capability of small frequency chirping and an efficient optical switch are discussed from the practical point of view.

I. INTRODUCTION

ONE OF the attractive features of quantum well (QW) structures is the existence of excitons at room temperature. The quantum confinement of the electrons and holes in the well layers makes the exciton binding energy and the oscillator strength of excitonic transitions larger than those of normal bulk crystals. Consequently, sharp and clearly-resolved exciton peaks have been observed in the room-temperature absorption spectra of several QW structures [1]–[4]. Excitonic nonlinear optical properties in QW structures, such as absorption saturation and the associated nonlinear refraction, have also been studied at room temperature [2], [5].

On the other hand, starting from two independent reports on the field effects of QW structures [6], [7], QW optical properties under the influence of the electric field perpendicular to the well plane have been extensively investigated. The field effects are attracting a great deal of practical interest due to their high potentiality for optical device applications. Up to now, several field-controlled optical devices such as a light emitter [7]–[11], electroabsorption modulator [12]–[15], optical bistable switch [16]–[18], and total-internal-reflection-switch [19] have

been proposed and/or demonstrated. One of the reasons these effects have such a great potential for optical device applications is their inherent capability for high-speed switching. For example, a short optical pulse less than 100 ps long was generated with a QW electroabsorption modulator [15]. Also, in our work [13], a switching of luminescence intensities from QW structures was observed to be completely free from lifetime limitations, resulting in about a 300 ps response time to a pulse-driving voltage. In both experiments, the RC time constant of the sample seems to limit the observed switching speed. The inherent switching time may in fact be much shorter than those reported.

In addition, the existence of room temperature excitons in QW structures increases the potentiality for practical application of the field effects. The QW optical properties relevant to the excitonic transition, such as the absorption coefficient and refractive index, can be sensitively affected by an electric field. As a result, by using the large field-induced variation of excitonic optical properties in QW structures, highly efficient field-controlled optical devices can be expected at room temperature. Actually, the electroabsorptive effect has been called the quantum-confined Stark effect (QCSE) [20]–[22] and plays an important role in a variety of electroabsorption modulators [12]–[15] and optical bistable switches [16], [17].

In the design of the field-controlled optical devices, it is very important to understand the electric-field effects on the QW optical properties. It may be considered that none of the aforementioned optical devices can be properly designed or investigated without sufficient data on the absorption coefficient and refractive index. Electroreflectance (ER) [23], [24] and electroabsorption (EA) [12] measurements are effectively available to understand the field effects on the refractive index and absorption coefficient of QW structures over a wide wavelength range, particularly involving the excitonic transition gap. However, thus far, there has been little systematic research reported that makes full use of the ER and EA measurements to investigate field-controlled optical devices. Particularly, no data on dispersion curves of the field-induced refractive index variation has been reported except for our own work [25]–[27].

In this paper, we shall report ER and EA data on AlGaAs QW structures at room temperature and the electric-field dependence of refractive index and absorption

Manuscript received February 17, 1987; revised August 28, 1987. This work was supported in part by a Scientific Research Grant-In-Aid for Specially Promoted Research from the Ministry of Education, Science and Culture of Japan.

Y. Kan, M. Yamanishi, and I. Suemune are with the Department of Physical Electronics, Faculty of Engineering, Hiroshima University, Sajio-cho, Higashi-hiroshima-shi, 724 Japan.

H. Nagai was with the Department of Physical Electronics, Hiroshima University, Sajio-cho, Higashi-hiroshima-shi, 724 Japan. He is now with the Matsushita Electric Industrial Co., Ltd., Osaka, Japan.

IEEE Log Number 8717464.

coefficient in more detail. Moreover, we shall discuss several possibilities for field-controlled optical devices based on the experimental data.

The structure of this paper is as follows. In Section II, we shall show ER spectra of a GaAs/AlAs multi-QW (MQW) structure at room temperature. The measured ER data can be well interpreted in terms of the theoretical dispersion of the refractive index variation, which includes the contributions of the excitonic transitions. The exciton-induced refractive index dispersions give a large variation rate of refractive index in response to field modulation at a photon energy near the lowest excitonic transition gap. In Section III, we shall report ER and EA spectra in a GaAs/AlGaAs MQW structure at room temperature, demonstrating a relation between the dispersion curves of the field-induced variations in the refractive index and absorption coefficient of the structure. In Section IV, we shall discuss the operation of the electroabsorption modulator and the total-internal-reflection switch according to the experimental and theoretical results of the field effects on the absorption coefficient and refractive index in QW structures. In Section V, we discuss conclusions derived from the research. The theoretical model and numerical parameters which are used in the calculation of the dispersions of refractive index- and absorption-variation due to the field effects are described in Appendix A. The contributions of the refractive index- and absorption-variations to reflectance modulation will be discussed in Appendix B. Appendix C presents an explanation of the dispersion curves induced by the refractive index variation due to the QCSE.

II. ELECTROREFLECTANCE MEASUREMENT

Electroreflectance (ER) measurements have been previously performed at room temperature to clarify the field effects on the refractive index of QW structures over a wavelength range particularly involving the excitonic transition gap [25], [27]. The sample configuration and experimental arrangements for the present ER measurements are shown in Fig. 1. N-doped Al_{0.7}Ga_{0.3}As (a thickness of ~1.0 μm) and a 20-period undoped MQW structure composed of alternating 100 Å GaAs wells and 300 Å AlAs barriers were sequentially grown on an n-type GaAs substrate by molecular beam epitaxy. The coupling between the adjacent wells in the MQW structure should be negligible because of the thick AlAs barriers, so that the structure can be regarded as a collection of uncoupled single QW's. Therefore, the theoretical estimations described through this paper were made by considering an isolated single QW structure.

A very thin (a thickness of ~200 Å) Au film, transmitting monochromatic light near the band edge at a rate of about 60 percent, was deposited on the top surface of the MQW structure to form a Schottky contact. The electric field across the MQW structure perpendicular to the well plane could be applied by reverse biasing the Schottky diode. It was confirmed by capacitance-voltage (C-V) measurements that the depletion layer completely

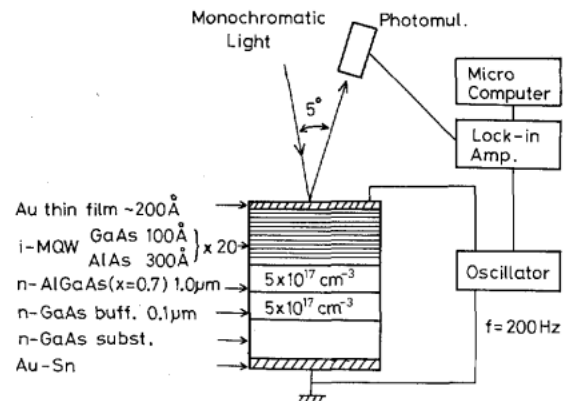


Fig. 1. Sample configuration and experimental arrangement used in the ER measurements.

spreads over the MQW structure for reverse bias voltages larger than 2 V, corresponding to an electric field of 3×10^4 V/cm. The applied field was modulated at a frequency of 200 Hz.

The light emitted from a halogen lamp was dispersed by a monochromator with a 1 nm resolution. The monochromatic light was focused on the surface of the sample under almost normal incidence (an incident angle of about 2.5°) and the reflected light intensity was measured by a photomultiplier. Only the modulated portion (proportional to the change in reflectivity) of the detected signals was amplified and detected with a lock-in amplifier. All the data were obtained at room temperature for low incident light intensities ($\sim 10^{-4}$ W/cm²), so that the intensity did not affect the obtained result.

Prior to description of the experimental results on the ER spectra, we show the theoretical dispersion of the field-induced variations of refractive index to aid in understanding the measured ER data. Fig. 2 shows the estimated dispersion of the field-induced variation in refractive index of the QW structure, for the same composition considered for the experimental situation shown in Fig. 1. The field applied to the QW structure was postulated to be modulated with a small amplitude (6.25×10^3 V/cm) at each bias field. The imaginary parts of dielectric constant caused by the excitonic- and free-carrier-transitions were estimated and their contributions to the real part of dielectric constant obtained by Kramers-Krönig transformation of the imaginary parts (see Appendix A). In the estimation, both energy- and polarization-dependent transition matrix elements in QW structures [28] and line broadening effects represented by the Gaussian line shape function were taken into account.

The lowest electron to heavy hole (1e1hh), the lowest electron to light hole (1e1lh) and the lowest electron to second heavy hole (1e2hh) transitions [29] contribute to the dispersion of the refractive index over the wavelength range as shown in Fig. 2. In the figure, the excitonic optical transition energies under each bias field are shown with arrows for each subband transitions. The theoretical energies of the 1e1hh and 1e1lh excitonic transitions almost agree with those of the longer and shorter wave-

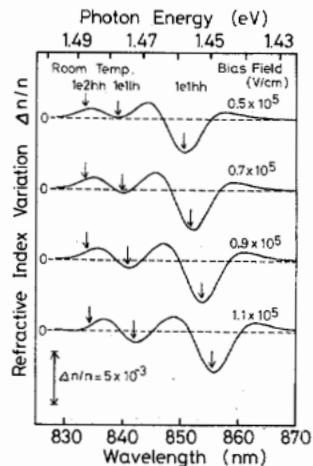


Fig. 2. Theoretical dispersion of the field-induced variation in the refractive index of the QW structure for several bias fields. The arrows show the theoretical excitonic transition energies of $1e1hh$, $1e1lh$, and $1e2hh$ transitions. The modulation field was assumed to be 6.25×10^3 V/cm.

length side downward peaks, respectively. The obtained dispersion curves result from the mixture of the shift of the excitonic transition energies and the change in the oscillator strength of the excitonic transitions due to the QCSE (see Appendix C).

Fig. 3 shows the measured ER spectra of the QW sample in Fig. 1 for a small modulating field of 6.25×10^3 V/cm and for various bias fields, which are conditions similar to those used for the calculated results shown in Fig. 2. Strictly speaking, both changes of the refractive index and of the absorption coefficient contribute to the reflectance variation $\Delta R/R$ which is directly obtained from the ER measurements. However, by using conventional formulations [30] for reflectance modulation due to refractive index- and absorption coefficient-variations, it was confirmed that the observed ER spectra are almost entirely dominated by refractive index-variation over the wavelength range of interest ($830 \sim 870$ nm) (see Appendix B). Thus, the ER spectra permit us to obtain a rough estimation of the dispersion of the refractive index variation $\Delta n/n$ by the following relation:

$$\Delta n/n = 0.75 \cdot (\Delta R/R). \quad (1)$$

The refractive index variation $\Delta n/n$ is simply proportional to the reflectance variation $\Delta R/R$, so that one can directly compare the experimental data in Fig. 3 with the theoretical results in Fig. 2 by suitably scaling the vertical axis in the figure. With respect to both the shapes and modulation depths of the dispersion curves, the observed ER data in Fig. 3 can be satisfactorily fitted by the theoretical curves in Fig. 2 which are dominated by the excitonic contribution at the excitonic transition gaps.

On the other hand, a similar calculation of the field-induced refractive index variation was also performed, in which the exciton contribution was ignored. The dispersion curves of refractive index variation in Fig. 4 show (a) the experimental spectrum obtained from the measured ER data, (b) the theoretical spectrum with exciton- and

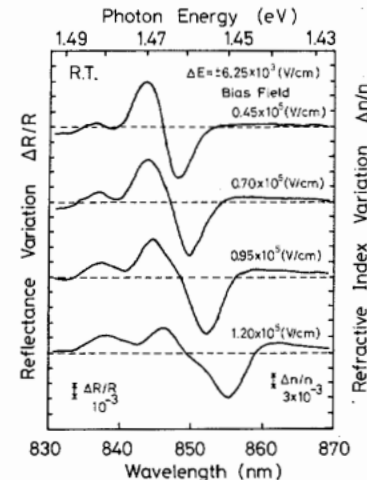


Fig. 3. Measured ER spectra for a small field modulation and for various bias fields at room temperature. The wavelength resolution was less than 1 nm. The fields were obtained from $C-V$ measurements.

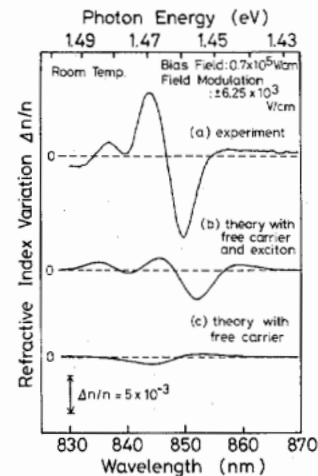


Fig. 4. Dispersion of the field-induced refractive index variation (a) obtained with ER measurements, (b) calculated with both exciton and free-carrier contributions, and (c) calculated with only the free-carrier contribution.

free-carrier-contributions, and (c) the theoretical spectrum with only the free-carrier contribution. As can be seen at a glance, the estimated dispersion curve of the refractive index variation of Fig. 4(c) is completely different from the measured curve [Fig. 4(a)], and the theoretical modulation depth is much smaller than that of the experimental result. This means that the excitonic transitions are crucially important for field-induced modulation of the refractive index in the GaAs/AlAs MQW structure at room temperature. Moreover, in spite of the significant red shifts of the downward peaks in Fig. 3, the fundamental shapes of the spectra were not seriously changed with increasing field up to 1.2×10^5 V/cm. This indicates that excitons in the MQW structure are quite stable under such a high field perpendicular to the well plane, even at room temperature. One of the reasons for the remaining discrepancy between the theoretical dispersion and the experiments with respect to the modulation depth of the refractive index may be attributed to uncertainty in

the value of exciton line width which sensitively affects the theoretical results.

The photon energies of the downward peaks in the ER spectra in Fig. 3 may be assignable to the $1e1hh$ and $1e1lh$ excitonic transitions energies for each bias field, judging from the good agreement between the theoretical (Fig. 2) and experimental (Fig. 3) spectral shapes. Red shifts of the downward peaks with increasing bias field are caused by field-induced carrier separation and the resultant perturbation of the energy levels of the confined particles in the well, combined with the reduction of the exciton binding energy. The shifted energies of the downward peaks as functions of the bias field are plotted in Fig. 5. The theoretical field-induced shifts of the $1e1hh$ and $1e1lh$ free carrier- and excitonic-transition energies are also shown in the figure. The free-carrier-transition energies were estimated by solving the one-dimensional Schrödinger equation, and the exciton binding energies were estimated by a variational technique for the trial exciton function [20], [21]. The observed peak shifts are well fitted to those of excitonic transitions rather than free-carrier transitions. This also supports the existence of room temperature excitons and their strong contribution to the ER spectra in QW structures with electric fields up to 1.2×10^5 V/cm. In addition, the agreement of the experiment with the theoretical estimation suggests that the assignment of the empirical electric field values was quite reasonable.

From the standpoint of device applications, it is important to know the variation of the refractive index induced by much larger field modulations. Fig. 6 shows the similarly measured ER spectra for large modulating fields at zero applied bias. The maximum variation in refractive index was deduced to be 4.4 percent in each QW from the measured value of the refractive index variation (1.1 percent) at the downward peak with photon energy of 1.455 eV for the variation in electric field (from 0 to 1.2×10^5 V/cm), taking the volume-ratio of the well to barrier layers into account. A maximum rate for the field-induced modulation of refractive index in each QW is deduced to be 3.7×10^{-9} m/V at photon energies close to the excitonic gap. The theoretical analysis on the refractive index changes due to an electric field application in QW structures has been reported by Yamamoto *et al.* [19]. But in their calculation, the exciton contribution was ignored and the reported theoretical ratio of the refractive index change to applied field was almost ten times smaller than the obtained value from our experiments. Their small ratio may be caused by the ignorance of exciton effects. It seems important to incorporate the exciton effects for the field-induced refractive index variation in QW structures.

The measured ER spectra described in this section indicate that room temperature excitons play a crucially important role in field-induced refractive index variations at photon energies close to the excitonic transition gaps in GaAs/AlAs MQW structures. The obtained large variation in refractive index may suggest the possibility of a field-controlled optical switch that is much more efficient

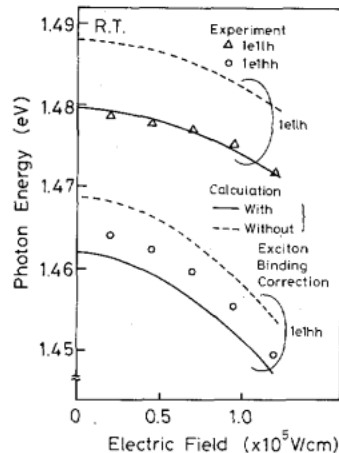


Fig. 5. Downward peak shifts in the ER spectra in Fig. 3 as a function of the bias field. The change in the estimated excitonic- (solid line) and free-carrier- (dashed line) transition energies for $1e1hh$ and $1e1lh$ transitions are also shown in the figure.

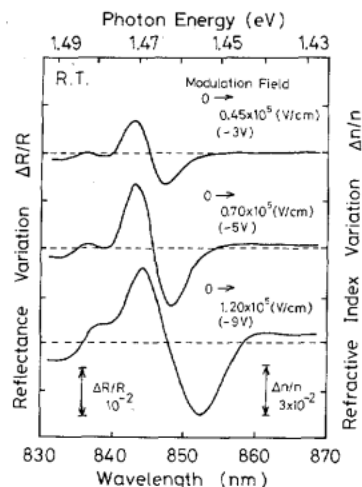


Fig. 6. ER spectra for large modulation fields at room temperature.

than the previous prediction [19]. This will be discussed in more detail in Section IV.

III. FIELD-INDUCED MODULATIONS OF REFRACTIVE INDEX AND ABSORPTION COEFFICIENTS

The variation of the QW absorption coefficient due to the QCSE is an important factor in considerations of the operational performance of the electroabsorption modulator [12]–[15]. On the other hand, as will be discussed in Section IV, the field-induced refractive index change has an undesirable effect on the modulation scheme [31]. Therefore, it is worthwhile to know not only the field-induced change in absorption coefficient but also the accompanying refractive index change. In this section, we shall investigate a relation between the dispersion curves of the field-induced variations in refractive index and absorption coefficient in a GaAs/AlGaAs QW structure with ER and EA measurements at room temperature [26], [27].

The ER and EA measurements were performed with the experimental arrangement and sample shown in Fig. 7. The sample has a 10-period undoped MQW structure con-

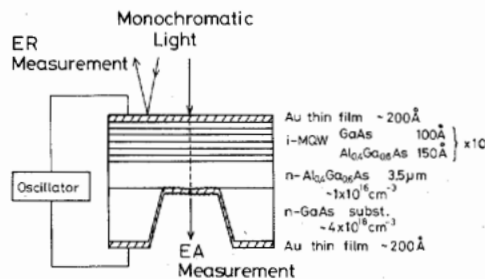


Fig. 7. Sample configuration used in the ER and EA measurements.

sisting of 100 Å GaAs wells and 150 Å Al_{0.4}Ga_{0.6}As barriers. A very thin (~200 Å) Au film was deposited on the top surface of the MQW structure to form a Schottky contact. A reverse bias voltage applied to the Schottky diode results in an electric field perpendicular to the well plane, across the MQW structure. Part of the opaque GaAs substrate was selectively etched away by chemical etching. The exposed surface of the n-AlGaAs layer was intentionally roughened by another chemical etching to prevent Fabry-Perot interference with the obtained result. Finally, the roughened surface was covered with a second deposited thin Au film.

The EA measurements were performed by measuring the intensity of monochromatic light beams transmitted through the central part of the sample. By contrast, the ER measurements for the same sample were performed at a spot outside the central hole of the substrate to avoid the influence of light reflected from the back surface of the sample. Experimental conditions, such as incident light intensity and frequency of the field modulation, were the same as those for the ER measurements described in the previous section (Section II).

The dispersion of the field-induced variations in the refractive index and absorption coefficient of the MQW structure, which were obtained with room-temperature ER and EA measurements, are shown in Fig. 8. It should be noted that the refractive index variation Δn shows a downward peak around the null-wavelength of the absorption variation $\Delta\alpha$, while $\Delta\alpha$ shows an upward peak around the null-wavelength of $\Delta n/n$.

The above-mentioned relation between Δn and $\Delta\alpha$ can be easily explained in terms of the relation between real and imaginary parts of the susceptibility near the resonance of a two-level system such as an exciton. Fig. 9(a) shows the theoretical exciton-induced dispersions of the refractive index and absorption coefficient near the excitonic transition energy. The dispersion curve of the refractive index is given by the Kramers-Krönig transformation of the absorption coefficient dispersion. When an electric field perpendicular to the well plane is applied to the QW structure, the refractive index and absorption coefficient vary, as shown in the figure, due to the field-induced shift of the excitonic gap and the variation of the oscillator strength of the exciton transition. The dispersion of the refractive index variation Δn and absorption coefficient variation $\Delta\alpha$ are given by the difference be-

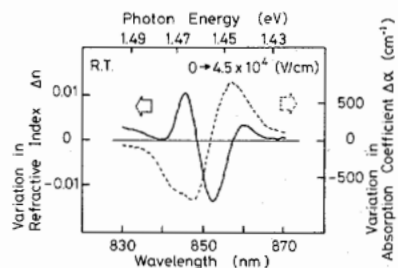
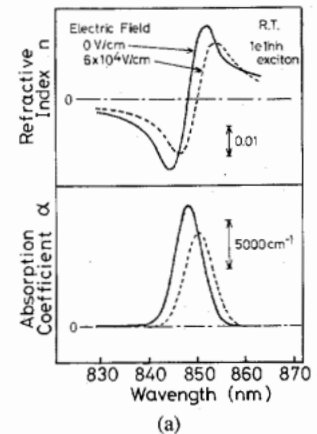
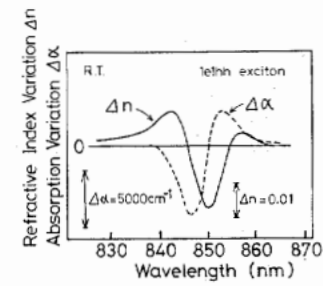


Fig. 8. Measured dispersion of the field-induced variation in the refractive index and absorption coefficient of a QW structure, obtained with ER and EA measurements at room temperature.



(a)



(b)

Fig. 9. (a) Theoretical exciton-induced dispersion of the refractive index and absorption coefficient near the lowest excitonic transition energy for zero field (0 V/cm) (solid line) and for a higher field of 6.0×10^4 V/cm (dashed line). (b) The theoretical relation between the field-induced refractive index variation (solid line) and the absorption variation (dashed line).

tween the solid and dashed lines in Fig. 9(a), as shown in Fig. 9(b). The relation between the theoretical Δn and $\Delta\alpha$ shown in Fig. 9(b) corresponds well to the measured relation shown in Fig. 8.

IV. DISCUSSION

The EA and ER measurements described in the previous section gave us considerable information on the electric-field dependence of refractive index and absorption coefficient in QW structures. The obtained results can be summarized as follows.

- 1) The room temperature exciton is quite stable in the AlGaAs MQW structure even under high fields (1.2×10^5 V/cm).
- 2) The maximum variation of the refractive index at a photon energy near the lowest excitonic transition gap was

obtained to be 4.4 percent in each QW, induced by the $1.2 \times 10^5 \text{ V/cm}$ field modulation.

3) A large field-induced variation of the absorption coefficient accompanied by no refractive index change is obtained at a specific wavelength. Also, a large refractive index variation is obtained with no absorption change at another specific wavelength.

In this section, we shall discuss the operating characteristics of the electroabsorption modulator and the total-internal-reflection switch based on the experimental and theoretical data of field effects on the absorption coefficient and refractive index in QW structures.

A. Electroabsorption Modulator

Several external electroabsorption modulators [12]–[15] using the field effect on the absorption coefficient in QW structures have been proposed, and high-speed operation of the devices has been demonstrated. From a practical viewpoint, one of the serious problems of the electroabsorption modulation scheme may be frequency chirping [31] caused by undesirable phase modulation due to a simultaneous refractive index change. The frequency chirping due to the phase modulation can be quantitatively expressed in terms of the α -parameter [31], defined as the ratio of the real to imaginary parts of the refractive index variation.

For example, the solid line in Fig. 10 shows the α -parameter estimated from the data on the absorption variation $\Delta\alpha$ and refractive index variation Δn in Fig. 8. Around the 857 nm wavelength, it is apparently possible to obtain a large absorption modulation with a very small α -parameter (almost 0). However, in practice, the electric field is not modulated with a step-like waveform, but rather, a finite transient time of the driving field exists. Consequently, the field applied to the QW structure in the modulator changes throughout the rising and decaying time of the field. Therefore, it is important to investigate the relation between the field-induced absorption variation and the refractive index variation at each moment of the field modulation including the transient region. In this case a more useful figure of merit is the parameter α' , defined as the ratio of the refractive index variation to the extinction coefficient variation caused by the small field modulation:

$$\alpha' = (dn/dE)/(dk/dE) \quad (2)$$

in which the extinction coefficient k is given by $k = \alpha\lambda/4\pi$ for absorption coefficient α . In practical applications of the field effect to an optical loss modulator, it is desirable to obtain a large field-induced variation of the absorption coefficient while keeping the α -parameter α' small over the entire range of applied modulation fields.

Figs. 11 and 12 show the theoretical α -parameter α' and the absorption coefficient at each wavelength, for wavelengths longer than the lowest excitonic gap wavelength at zero field, as a function of the applied field in a GaAs/AlAs QW structure (with a well thickness of 110 Å), respectively. As described in Appendix C, the null-

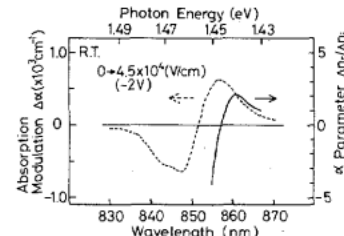


Fig. 10. Calculated α -parameter from the experimental data on $\Delta\alpha$ and Δn in Fig. 8. The measured dispersion of the field-induced absorption variation is also shown by the dashed line.

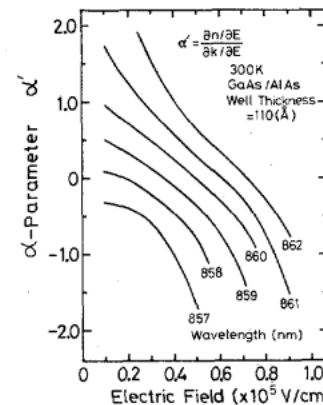


Fig. 11. Theoretical α' -parameter α' at each wavelength as a function of applied field in a GaAs/AlGaAs QW structure with a well thickness of 110 Å.

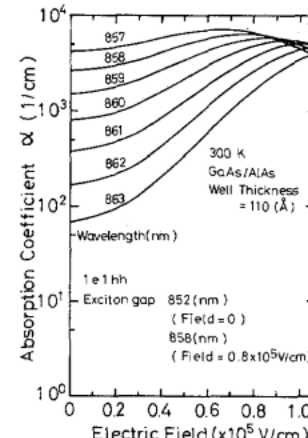


Fig. 12. Theoretical absorption coefficient in a GaAs/AlAs QW structure at each wavelength as a function of applied field. The considered structure of the QW is the same as that of Fig. 11.

wavelength of the refractive index variation due to the field effects will be realized at a particular wavelength longer than the excitonic gap. Therefore, a very useful wavelength, where the absorption variation is available with a very small refractive index variation, may exist on the long wavelength side of the lowest excitonic gap. For example, at a wavelength of 862 nm, the absorption coefficient changes from 300 to 3600 cm^{-1} for a variation in the electric field from 0.3 to $0.9 \times 10^5 \text{ V/cm}$, while the absolute value of the α -parameter α' is kept to values less than 1.0 over almost the entire range of the field modulation. Strictly speaking, nonzero α' will cause unnece-

sary broadening for signals transmitted through an external modulator. However, the value $\alpha' = 1$ is much less than the measured one for direct modulation of an injection laser diode (~ 3) [32], and it may be small enough for device applications. Assuming a loss modulator with a $10 \mu\text{m}$ effective pass length ΓL (Γ = confinement factor, L = length of the modulator), the absorption loss can then be modulated from 1.3 to 16 dB for the above field modulation, resulting in a sufficient modulation depth (on/off ratio of 12:1). The effective α -parameter α_{eff} caused by the field modulation may be estimated as an average of α' over the electric field range

$$\alpha_{\text{eff}} = \left\{ \frac{1}{E_2 - E_1} \int_{E_1}^{E_2} |\alpha'(E)|^2 dE \right\}^{1/2} \quad (3)$$

The parameter α_{eff} is estimated to be 0.70 for field modulation from 0.3 to $0.9 \times 10^5 \text{ V/cm}$ at a wavelength of 862 nm. This indicates that one might realize an effective electroabsorption modulator almost free from frequency chirping, by properly choosing the operating wavelength. In fact, very recently, such a small α -parameter (~ 1.0) in a GaAlAs QW electroabsorption modulator has been experimentally demonstrated by Wood *et al.* [33].

B. Total-Internal-Reflection Switch

One possible device application of the field-induced refractive index variation in QW structures is the total-internal-reflection switch with two waveguides crossing each other [19]. In [19], the refractive index variation due to an electric field applied to the QW was analyzed and the optical switch was discussed based on the theoretical result. In their calculation, the contribution of the excitonic transition was neglected. However, as described in Section II, we experimentally confirmed that the exciton

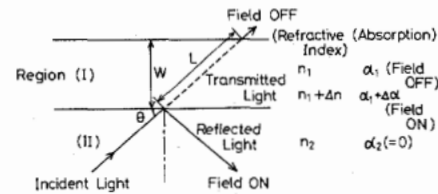


Fig. 13. Top view of the total-internal-reflection waveguide switch using the field effect on the refractive index of QW structures.

region (I) results in the total-internal-reflection of the incident light. Here, it is assumed that the refractive index and absorption coefficient in region (I) without the field are denoted n_1 and α_1 , respectively, and the parameters change to $n_1 + \Delta n$ and $\alpha_1 + \Delta \alpha$ with field application. Also, it is assumed that region (II) has a refractive index of n_2 ($= n_1$) and no absorption loss. Incident light goes straight through regions (I) and (II) under the no field condition. When an electric field perpendicular to the plane of the paper is applied to the QW structure in region (I), a dielectric boundary is formed by a corresponding decrease in the refractive index of region (I), reflecting the incident light. In the present scheme, two kinds of optical loss must be taken into account. One is the absorption loss which affects the light propagating through region (I) under the no field condition. The product of the light pass length L , which is given by $L = W/\sin \theta$ (θ is the propagation angle with respect to the dielectric boundary), and the absorption coefficient α_1 in region (I) may directly affect the amplitude of the optical output. The second kind is the loss associated with the reflection. The power reflectivity R for light incident at the dielectric interface in Fig. 13 is given by the following Fresnel equation for the complex reflectivity including the absorption loss in region (I):

$$R = \left| \frac{(n_1 + \Delta n - ik_1) \cos \theta_i - n_2 \sqrt{1 - \left(\frac{n_2}{n_1 + \Delta n - ik_1} \right)^2 \sin^2 \theta_i}}{(n_1 + \Delta n - ik_1) \cos \theta_i + n_2 \sqrt{1 - \left(\frac{n_2}{n_1 + \Delta n - ik_1} \right)^2 \sin^2 \theta_i}} \right|^2 \quad (4)$$

in AlGaAs QW structures is quite stable even under high field at room temperature, and that the existence of such excitons is crucially important for the large field-induced variation of the refractive index in the structure. Here, we shall reexamine the device characteristics of the total-internal-reflection switch by including field effects on the excitonic transitions. Furthermore, in the optical switch, any modulation of the absorption coefficient in the QW structure may affect the device characteristics. Therefore, not only the electric-field dependence of the refractive index, but also the effect of the absorption loss should be considered.

The top view of the proposed total-internal-reflection switch [19], which is operated in a waveguide configuration, may be simply represented as shown schematically in Fig. 13. The field-induced refractive index variation in

which the various notations correspond to the parameter in Fig. 13 with the following relations:

$$\theta_i = 90^\circ - \theta \quad (5)$$

and

$$k_1 = \lambda(\alpha_1 + \Delta \alpha)/4\pi. \quad (6)$$

Fig. 14 shows the reflectivity R as a function of the propagation angle θ calculated by using (4). A large refractive index variation and a small absorption loss are required to keep the reflectivity large and the reflection loss small. We shall investigate the device properties for two kinds of QW structures.

Fig. 15 shows (a) the field-induced refractive index variation and (b) the absorption coefficient dispersion for

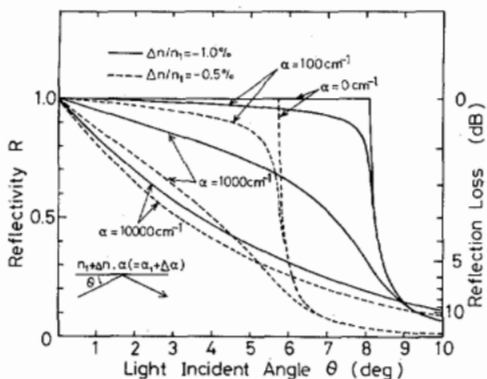


Fig. 14. Calculated power reflectivity R at the dielectric interface as a function of the light incident angle θ measured from the boundary plane. The quantities $n_1 + \Delta n$ and $\alpha_1 + \Delta \alpha$ correspond to the refractive index and absorption coefficient in region (I) in Fig. 13 under applied field conditions, respectively.

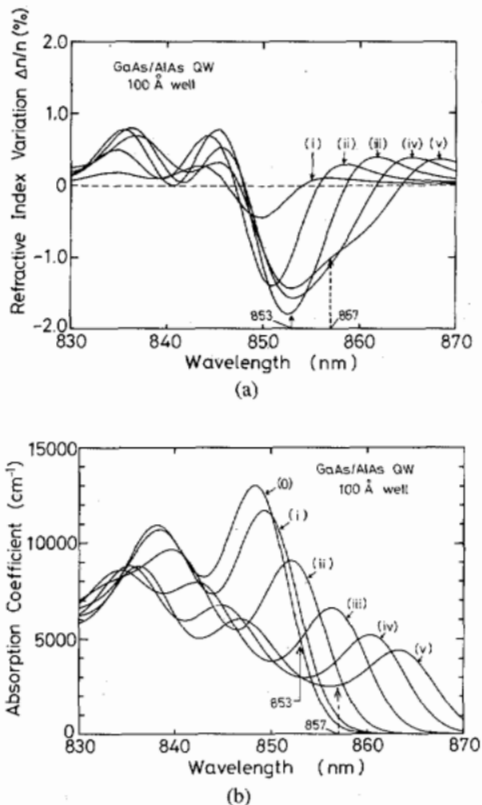


Fig. 15. Theoretical dispersion of (a) the field-induced refractive index variation for a field modulation from 0 to (i) 0.4×10^5 , (ii) 0.8×10^5 , (iii) 1.2×10^5 , (iv) 1.5×10^5 , and (v) 1.7×10^5 V/cm, and (b) the absorption coefficient under an applied field of (0) 0, (i) 0.4×10^5 , (ii) 0.8×10^5 , (iii) 1.2×10^5 , (iv) 1.5×10^5 , and (v) 1.7×10^5 V/cm. The calculations were carried out for a GaAs/AlAs QW structure with a well thickness of 100 Å.

each applied field, which are calculated by considering a GaAs/AlAs QW structure with a well thickness of 100 Å as in region (I) in Fig. 13. For a variation in the electric field from 0 to 1.2×10^5 V/cm, a maximum change in the refractive index of 1.8 percent may be expected at the 853 nm wavelength (indicated by the solid arrow in Fig. 15). However, in this case, the associated large absorption coefficient of 5000 cm^{-1} without applied field seri-

ously affects the device characteristics. Under these conditions, the incident angle θ may be chosen to be about 6.0° , which yields a significant reflectivity R (0.5). The optical loss for light propagating through region (I) without field is estimated to be 10 dB, supposing that the width of region (I) is 1 μm and that the confinement factor of the region is 0.5.

The serious influence of the absorption loss under the field-off condition may be avoided if the wavelength is chosen to be far longer than the excitonic gap at zero field. In this case, a comparatively higher field will be required to provide significant reflection under the field-on condition. For instance, at the wavelength of 857 nm (indicated by the dashed arrow in Fig. 15), where the absorption coefficient without field is as small as 450 cm^{-1} , a refractive index variation of 1.1 percent with an absorption coefficient of 2500 cm^{-1} may be expected for a field modulation of 1.7×10^5 V/cm. For these conditions, a reflectivity of 0.5 (which corresponds to a 3 dB reflection loss) will be obtained at a light-incident angle of about 4° , while the transmission loss without field is 1.4 dB. The resulting light angle of 4° , which corresponds to an 8° crossing angle of the two waveguides in the optical switch, may be reasonable for practical device applications. Actually, an optical switch which had two waveguides crossing at an angle of 7° , was demonstrated based on the band-filling effect in an InGaAsP/InP semiconductor waveguide [34]. The switching time of the present total-internal-reflection switch based on the electric-field effects in QW structures is expected to be much shorter than that of the device in [34], for which the carrier lifetime effectively limits the switching speed.

Fig. 16 shows the theoretical refractive index variation and the absorption coefficient for a GaAs/AlAs QW structure with a 140 Å-width well. In this case, one might expect to obtain device operation with a small loss by use of a smaller field modulation than that used in the former case. Electric field effects both on the excitonic transition energies and on the oscillator strength of the excitonic transitions are caused by the field-induced separation of electrons and holes. The more the well thickness of QW structures is widened, the more electrons and holes separate due to an electric field application. Consequently, one can expect larger field effect for QW structures with a wide well than for those with a narrow well [35], [36] as follows. Even if an absorption-free wavelength far from the lowest excitonic gap at zero field is chosen, a large refractive index variation due to the large field-induced red shift of the excitonic transition energy can be expected. In addition, the applied field makes the oscillator strength of the excitonic transition small so that the influence of the absorption under field-on conditions can be lowered.

When the incident light wavelength is adjusted to 868 nm (as indicated by the arrow in Fig. 16), low loss operation of the device may be expected for field modulation ranging from 0 to 1.0×10^5 V/cm. At this wavelength, a sufficient refractive index variation per one well ($\Delta n/n$)

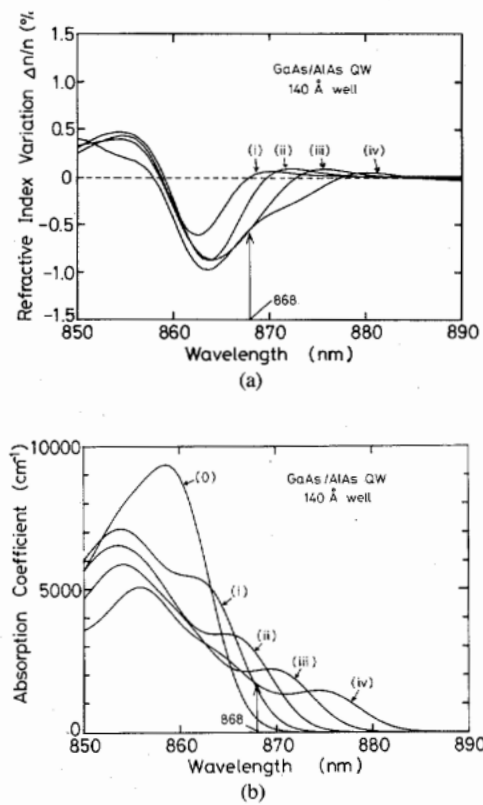


Fig. 16. Theoretical dispersion of (a) the field-induced refractive index variation for a field modulation from 0 to (i) 0.4×10^5 , (ii) 0.6×10^5 , (iii), 0.8×10^5 , and (iv) $1.0 \times 10^5 \text{ V/cm}$, and (b) the absorption coefficient under an applied field of (0) 0, (i) 0.4×10^5 , (ii) 0.6×10^5 , (iii) 0.8×10^5 , and (iv) $1.0 \times 10^5 \text{ V/cm}$. The calculations were performed for a GaAs/AlAs QW structure with a well thickness of 140 Å.

$= 0.55$ percent) is available while the undesirable absorption is considerably reduced [absorption coefficients: $\alpha_1 = 400 \text{ cm}^{-1}$ without field, $\alpha_1 + \Delta\alpha = 1600 \text{ cm}^{-1}$ with field in Fig. 16(b)]. The reflection loss will be 3 dB at an incident angle of 3° , while the transmission loss for propagating light under the field-off condition is about 2.3 dB, supposing that the width of region (I) is $1 \mu\text{m}$. In this estimation, a confinement factor of 0.7 was assumed by considering a MQW structure composed of 140 Å GaAs wells and 60 Å AlAs barriers. The barrier may be thick enough to confine the carriers into wells and to prevent coupling between the adjacent wells. In the 140 Å well case described here, one might expect to obtain device operation with a small loss by use of a smaller field modulation than that used in the 100 Å well case.

As described in this section, the absorption of QW structures with and without field seriously affects the characteristics of the total-internal-reflection switch. Both the transmission and reflection losses of the device operating at 857 nm for a 100 Å well-QW structure and at 868 nm for a 140 Å well-QW structure were calculated as functions of the incident light angle, and are summarized in Fig. 17. The parameters used in the calculation are shown in the figure. The parameter Γ denotes a confinement factor and n_1 , Δn , α_1 , and $\Delta\alpha$ correspond to the notations in Fig. 13. The width of region (I) in Fig. 13

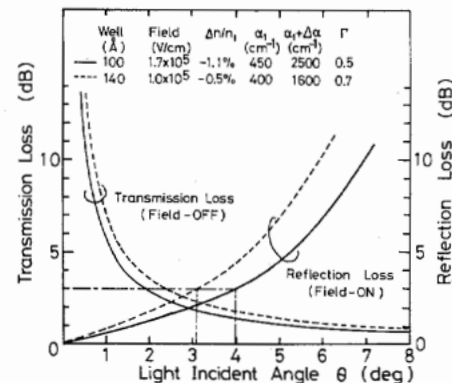


Fig. 17. Theoretical losses for incident light intensities in the total-internal-reflection switch. Reflection loss in the field-on condition and transmission loss in the field-off condition are calculated as a function of incident angle measured from the dielectric boundary. GaAs/AlAs QW's with a well thickness of 100 (solid line) and of 140 Å (dashed line) were considered. The parameters used in the calculation are shown in the figure.

was assumed to be $1 \mu\text{m}$. In both QW structures, the operational wavelength must be carefully chosen to optimize the device characteristics.

V. CONCLUSION

In conclusion, we have measured ER spectra for a GaAs/AlAs MQW structure at room temperature. The measured ER data have been well interpreted in terms of the theoretical dispersion of the refractive index variation, which involves contributions from the excitonic transitions. It has been concluded that the excitonic transitions are mainly responsible for the variations in the refractive index. A maximum variation of the refractive index $\Delta n/n$ in each QW at a photon energy near the lowest excitonic transition gap was obtained to be 4.4 percent, induced by a $1.2 \times 10^5 \text{ V/cm}$ field modulation. We have also shown ER and EA spectra in a GaAs/AlGaAs MQW structure at room temperature, demonstrating a relation between dispersion curves of the field-induced variations in refractive index and absorption coefficient in the structure. The field-induced absorption variation exhibits peaks around the null-wavelength of the refractive index variation.

Based on the experimental and theoretical results, we have discussed two kinds of field-controlled optical devices. The results indicate the possibility of an electroabsorption modulator almost free from frequency chirping, operating at a particular photon energy below the excitonic gap. Effective operation of the total-internal-reflection waveguide switch with small optical losses has been also examined. However, in both kinds of optical devices, device characteristics sensitively depend on operational conditions such as the light wavelength and the thickness of the QW's. Therefore, it is required to precisely adjust the parameters of the optimum condition. On the other hand, the composition of the QW structure also strongly influences the device operation. Consequently, it will be very important to fabricate the QW structure as designed. Accurately controlled epitaxial growth techniques, such as phase-locked epitaxy [37] and migration-

enhanced epitaxy [38], may be effectively adopted for fine control of the QW structures.

APPENDIX A

THEORETICAL ESTIMATION OF ELECTRIC-FIELD EFFECTS ON THE REFRACTIVE INDEX AND ABSORPTION COEFFICIENT IN QW STRUCTURES

We estimated the electric-field dependence of the refractive index and the absorption coefficient in QW structures with the following theoretical method. The imaginary parts of the dielectric constant caused by the excitonic- and free-carrier-transitions were estimated, and then, their contributions to the real part of the dielectric constant were obtained by the Kramers-Krönig transformation of the imaginary parts. The theoretical dispersions of the absorption coefficient and the refractive index were obtained from the imaginary and real parts of the estimated dielectric constant, respectively.

In the estimation of the free-carrier contribution, energy- and polarization-dependent momentum matrix elements [28] and line broadening represented by a Gaussian line shape function were taken into account. The contributions of free-carrier-transitions to the imaginary part may be written

$$\epsilon_i(\hbar\omega) = \frac{e^2}{\epsilon_0 m_0^2 \omega^2 L_z} \frac{m_{eh}}{\pi \hbar^2} \sum_i \sum_j |M_b|^2 \cdot \left| \int \psi_{ei}(z) \psi_{hj}(z) dz \right|^2 \cdot \int M(E) F(E + E_g + E_{ei} + E_{hj} - \hbar\omega) dE \quad (A.1)$$

in which L_z is the thickness of the QW, m_{eh} is the reduced hole effective mass E_g , E_{ei} and E_{hj} are the energy gap, and the quantized energies of the $n = i$ electron and $n = j$ hole, respectively, and $\hbar\omega$ denotes the photon energy. The energies E_{ei} and E_{hj} , and the $n = i$ electron and $n = j$ hole wave functions $\psi_{ei}(z)$ and $\psi_{hj}(z)$, respectively, are solutions of the one-dimensional Schrödinger equations for the QW subjected to the electric field [39]. The quantity $|M_b|^2$ is the average matrix element for the Bloch state [40] given by

$$|M_b|^2 = \frac{m_0^2 E_g (E_g + \Delta)}{12 m_e (E_g + \frac{2}{3}\Delta)} \quad (A.2)$$

in which m_e is the electron effective mass and Δ the spin orbit split-off energy. The theoretical matrix elements derived on the basis of $k \cdot p$ perturbation theory may result in an underestimation. For example, the absorption coefficient calculated by the use of $|M_b|^2$ given by (A.2) is too small by a factor of approximately $1.5 \sim 2.1$ compared with experimental values [41]. Therefore, we used a value for $|M_b|^2$ two times as large as the one given by (A.2).

In (A.1), $F(\hbar\omega_0 - \hbar\omega)$, ($\hbar\omega_0 = E + E_g + E_{ei} + E_{hj}$),

is the Gaussian line shape function defined as

$$F(\hbar\omega_0 - \hbar\omega) = \frac{1}{\sqrt{\pi\delta}} \exp \left\{ -(\hbar\omega_0 - \hbar\omega)^2 / \delta^2 \right\} \quad \delta = h/\tau(\ln 2)^{-1/2}. \quad (A.3)$$

The energy dependence of the energy- and polarization-dependent transition matrix elements [28] are given by the following equations:

$$M(E) = \frac{3}{4} (1 + \cos^2 \theta) = \frac{3}{4} \left(1 + \frac{E_{ei} + E_{hj}}{E_{ei} + E_{hj} + E} \right) \quad \text{(for electron to heavy hole transitions)} \quad (A.4)$$

$$M(E) = \frac{1}{4} (5 - 3 \cos^2 \theta) = \frac{1}{4} \left(5 - 3 \frac{E_{ei} + E_{hj}}{E_{ei} + E_{hj} + E} \right) \quad \text{(for electron to light hole transitions)} \quad (A.5)$$

in which θ is the angle of the electron wave vector with respect to the z axis (normal to the well plane), and the polarization is assumed to be parallel to the plane of the layers (TE-mode).

On the other hand, the contributions of the excitonic transitions may be written

$$\epsilon_i(\hbar\omega) = \frac{2\pi e^2}{\epsilon_0 m_0^2 \omega^2 L_z} \frac{3}{2} |M_b|^2 |\phi_{ex}(0)|^2 \cdot \left| \int \psi_{ei}(z) \psi_{hj}(z) dz \right|^2 \cdot F(\hbar\omega_{ex} - \hbar\omega) \quad \text{(for heavy hole exciton)} \quad (A.6)$$

$$\epsilon_i(\hbar\omega) = \frac{2\pi e^2}{\epsilon_0 m_0^2 \omega^2 L_z} \frac{1}{2} |M_b|^2 |\phi_{ex}(0)|^2 \cdot \left| \int \psi_{ei}(z) \psi_{hj}(z) dz \right|^2 \cdot F(\hbar\omega_{ex} - \hbar\omega) \quad \text{(for light hole exciton)} \quad (A.7)$$

in which the momentum matrix elements [28] for the TE mode are taken into account and $\hbar\omega_{ex}$ denotes the excitonic transition energy. The exciton binding energy E_{exb} , which is included in $\hbar\omega_{ex}$, and the proportional term of the oscillator strength of the excitonic transition $|\phi_{ex}(0)|^2 \cdot |\int \psi_{ei}(z) \psi_{hj}(z) dz|^2$ were estimated by a variational technique for the trial exciton function [20], [21], [39],

$$\phi_{ex}(r) = \frac{(2/\pi)^{1/2}}{\lambda} \exp(-r/\lambda). \quad (A.8)$$

In the numerical estimation, the following numerical

parameters reasonable for MQW structures were used [36], [42]: electron effective mass $m_e = (0.0665 + 0.0835x)m_0$; heavy hole effective masses $m_{hh\perp} = (0.34 + 0.42x)m_0$, $m_{hh\parallel} = 0.1m_0$ for perpendicular and parallel to the well plane, respectively; light hole effective masses $m_{lh\perp} = (0.094 + 0.043x)m_0$, $m_{lh\parallel} = 0.2m_0$ for perpendicular and parallel to the well plane, respectively, where x is the Al-mole fraction of AlGaAs barrier layers; the spin orbit split-off energy $\Delta = 0.33$ eV; a 60:40 split ratio for band discontinuities in the conduction and valence bands; and the full width at half maximum of the Gaussian function is 13 meV.

APPENDIX B

CONTRIBUTIONS OF THE REFRACTIVE INDEX- AND ABSORPTION COEFFICIENT-VARIATION TO THE REFLECTANCE MODULATION

The dispersion of the reflectance is given by [30]

$$\Delta R/R = \alpha\Delta\epsilon_1 + \beta\Delta\epsilon_2 \quad (B.1)$$

assuming that the dielectric constant $\epsilon = \epsilon_1 + i\epsilon_2$ is modulated by amounts $\Delta\epsilon_1$ and $\Delta\epsilon_2$. The coefficients α and β are expressed in a mixed notation:

$$\alpha = 2\gamma/(\gamma^2 + \delta^2) \quad (B.2)$$

$$\beta = 2\delta/(\gamma^2 + \delta^2) \quad (B.3)$$

$$\gamma = n(n^2 - 3k^2 - 1) \quad (B.4)$$

$$\delta = k(3n^2 - k^2 - 1) \quad (B.5)$$

in which n and k are the refractive index and the extinction coefficient in MQW structures. The extinction coefficient k is related to the absorption coefficient α_a by the following equation:

$$k = \alpha_a\lambda_0/4\pi \quad (B.6)$$

in which λ_0 is the wavelength in free space.

The values of the coefficients α , β , γ , and δ are obtained to be 6.11×10^{-2} , 4.02×10^{-3} , 32.6, and 2.14, respectively, by assuming the absorption coefficient and the refractive index around the wavelength of the excitonic gap to be 10^4 cm $^{-1}$ and 3.3, respectively. Then, k is obtained to be 6.76×10^{-2} for the wavelength λ_0 of 850 nm. On the other hand, the real part ϵ_1 and the imaginary part ϵ_2 of dielectric constant are related to the refractive index n and the extinction coefficient k by the following equation:

$$\epsilon_1 = n^2 - k^2 \quad (B.7)$$

$$\epsilon_2 = 2nk. \quad (B.8)$$

From equations (B.6), (B.7), and (B.8), the variations of ϵ_1 and ϵ_2 are given by

$$\Delta\epsilon_1 = 2(n\Delta n - k\Delta k) \sim 2n\Delta n \quad (B.9)$$

$$\begin{aligned} \Delta\epsilon_2 &= 2(n\Delta k + k\Delta n) \sim 2n\Delta k \\ &= (\lambda_0 n/2\pi) \cdot \Delta\alpha \end{aligned} \quad (B.10)$$

in which terms involving k are neglected because k is much smaller than n in the present situation.

For example, assuming the refractive index variation Δn close to the lowest exciton gap to be as small as $0.01n$ from the experimental data for the smallest field modulation case in Fig. 6, and the absorption coefficient variation $\Delta\alpha$ also close to the lowest exciton gap to be as large as 5×10^3 cm $^{-1}$ estimated from the theoretical absorption coefficient for each bias field as shown in Fig. 15(b), $\Delta\epsilon_1$ and $\Delta\epsilon_2$ are obtained to be $\Delta\epsilon_1 \sim 0.218$ and $\Delta\epsilon_2 \sim 0.223$ from (B.9) and (B.10). Although the variation of the imaginary part of the dielectric constant $\Delta\epsilon_2$ is almost the same as the variation of the real part $\Delta\epsilon_1$, the coefficient β is less than one-tenth of α . Even in the assumption that the large $\Delta\alpha$ may effect the reflectance variation ΔR , the influence of the second term on the reflectance modulation $\Delta R/R$ is less than 10 percent of the first term in (B.1) and may be neglected to obtain

$$\Delta R/R \sim \alpha\Delta\epsilon_1. \quad (B.11)$$

Also, under the above condition, δ is much smaller than γ so that α is given from (B.2) and (B.4):

$$\alpha \sim 2/\gamma \sim 2/\{n(n^2 - 1)\}. \quad (B.12)$$

From (B.9), (B.11), and (B.12),

$$\frac{\Delta R}{R} \sim \frac{2}{n(n^2 - 1)} 2n\Delta n \quad (B.13)$$

$$\begin{aligned} \frac{\Delta n}{n} &= \frac{n^2 - 1}{4n} \frac{\Delta R}{R} \\ &= 0.75 \cdot \Delta R/R \end{aligned} \quad (B.14)$$

using $n = 3.3$.

For example, from Fig. 6 in Section II, the reflectance variation $\Delta R/R$ is obtained to be about 1.4 percent at a photon energy of 1.455 eV. The refractive index variation $\Delta n/n$ can be deduced to be about 1.1 percent by using the relation given in (B.13). The obtained value of $\Delta n/n$ is the averaged refractive index variation of the volume-ratio of the well thickness (100 Å) to barrier thickness (300 Å); it is concluded that a refractive index variation of 4.4 percent may be induced in each QW due to the applied field:

$$\begin{aligned} \Delta n/n &= 1.1 \times \frac{100 + 300}{100} \sim 4.4 \text{ percent} \\ &\quad (\text{per one well}). \end{aligned} \quad (B.15)$$

The variation rate of the refractive index for the electric field modulation $\Delta n/n/E$ is given by

$$\begin{aligned} \Delta n/n/E &= 4.4 \times 10^{-2}/(1.2 \times 10^5) \\ &\sim 3.7 \times 10^{-9} \text{ (m/V)}. \end{aligned} \quad (B.16)$$

APPENDIX C FIELD-INDUCED REFRACTIVE INDEX VARIATION

The dispersion of the field-induced refractive index variation can be explained as follows. The exciton reso-

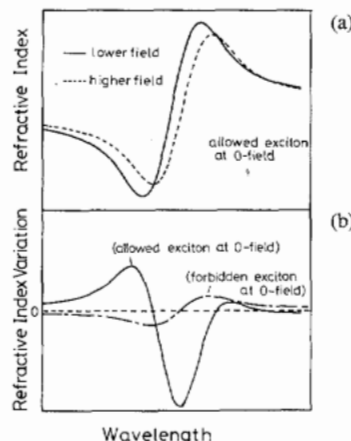


Fig. 18. Schematic drawings of (a) the refractive index dispersion near the lowest exciton gap, allowed at $E = 0$, under lower field (solid line) and higher field (dashed line) and (b) the field-induced refractive index variation of $1e1hh$ or $1e1lh$ (solid line) transitions and $1e2hh$, forbidden at the $E = 0$ (dot-dashed line) transition near each excitonic gap at the bias field used for the modulation.

nance induces a dispersion of the refractive index near the excitonic transition energy as shown in Fig. 18(a) with a solid line. When an electric field perpendicular to the well plane is applied to the QW structures, the excitonic transition energies and the oscillator strength change due to the QCSE as shown in Figs. 19 and 20, respectively. As a result, for the lowest electron to heavy hole excitonic transition ($1e1hh$), the dispersion curve of the refractive index shifts to the longer wavelength side and its amplitude is reduced with increasing field [shown by a dashed line in Fig. 18(a)]. The spectrum of the field-induced refractive index variation Δn is given by the difference between the solid and dashed lines in Fig. 18(a) as shown in (b) with a solid line. The energy at the downward peak of Δn almost agrees with the excitonic transition energy at the bias field employed for the small field-modulation.

The field-induced variation of refractive index for the lowest electron to light hole excitonic transition ($1e1lh$) can be similarly considered. However, the refractive index dispersion for the lowest electron to second heavy hole excitonic transition ($1e2hh$) behaves differently under the influence of the electric field. The $1e2hh$ transition is forbidden under zero field conditions in the QW structure and its oscillator strength increases with increasing field, as shown in Fig. 20. The dispersion of the refractive index variation related to the $1e2hh$ excitonic transition is given by the dot-dashed line in Fig. 18(b).

ACKNOWLEDGMENT

The authors wish to express their thanks to Dr. Y. Ide and Dr. R. Lang, Opto-Electronics Research Laboratories, NEC Corporation, and Dr. T. Hijikata and Dr. T. Hayakawa, Central Research Laboratory, Sharp Corporation, for kindly supplying the GaAlAs wafer used in the work and for stimulating discussions; and Y. Lee, Y. Funahashi, and M. Kurosaki for the numerical calculations employed in the theoretical work.

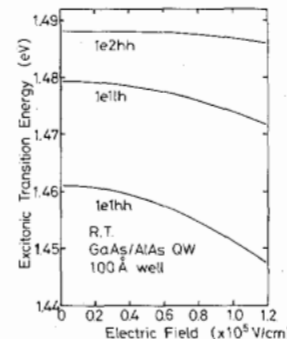


Fig. 19. Theoretical field-induced shifts of the excitonic transition energies for $1e1hh$, $1e1lh$, and $1e2hh$ transitions in a GaAs/AlAs QW structure with a well thickness of 100 Å.

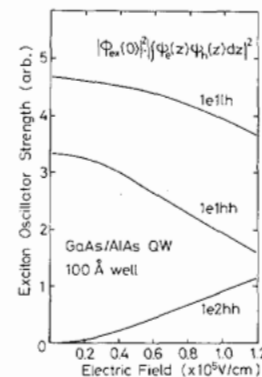


Fig. 20. Theoretical field-induced changes in the oscillator strength of the excitonic transition for the $1e1hh$, $1e1lh$, and $1e2hh$ transitions in a GaAs/AlAs QW structure with a well thickness of 100 Å. The changes in the proportional term of the oscillator strength are shown.

REFERENCES

- [1] T. Ishibashi, S. Tarucha, and H. Okamoto, "Exciton associated optical absorption spectra of AlAs/GaAs superlattices at 300 K," in *Proc. Int. Symp. GaAs Related Compounds, Inst., Phys. Conf.*, Japan, no. 63, pp. 587-588, 1981.
- [2] D. A. B. Miller, D. S. Chemla, D. J. Eilenberger, P. W. Smith, A. C. Gossard, and W. T. Tsang, "Large room-temperature optical nonlinearity in GaAs/ $Ga_{1-x}Al_xAs$ multiple quantum well structures," *Appl. Phys. Lett.*, vol. 41, pp. 679-681, 1982.
- [3] J. S. Weiner, D. S. Chemla, D. A. B. Miller, T. H. Wood, D. Sivco, and Y. Cho, "Room temperature excitons in 1.6-μm band-gap GaInAs/AlInAs quantum wells," *Appl. Phys. Lett.*, vol. 46, pp. 619-621, 1985.
- [4] T. Miyazawa, S. Tarucha, Y. Ohmori, Y. Suzuki, and H. Okamoto, "Observation of room temperature exciton in GaSb-AlGaSb multi-quantum wells," *Japan. J. Appl. Phys.*, vol. 25, pp. L200-L202, 1986.
- [5] D. S. Chemla, D. A. B. Miller, P. W. Smith, A. C. Gossard, and W. Wiegmann, "Room temperature excitonic nonlinear absorption and refraction in GaAs/AlGaAs multiple quantum well structures," *IEEE J. Quantum Electron.*, vol. QE-20, pp. 265-275, 1984.
- [6] E. E. Mendez, G. Bastard, L. L. Chang, L. Esaki, H. Morkoc, and R. Fisher, "Effect of an electric field on the luminescence of GaAs quantum wells," *Phys. Rev. B*, vol. 26, pp. 7101-7104, 1982.
- [7] M. Yamanishi and I. Suemune, "Quantum mechanical size effect modulation light sources—A new field effect semiconductor laser or light emitting device," *Japan. J. Appl. Phys.*, vol. 22, pp. L22-L24, 1983.
- [8] M. Yamanishi, H. Yamamoto, and I. Suemune, "Size effect modulation light sources—Possibility of LED mode operation at room temperature," *Superlattices Microstruct.*, vol. 1, pp. 335-337, 1985.
- [9] Y. Kan, M. Yamanishi, Y. Usami, I. Ogura, and I. Suemune, "Life time-free switching of luminescence from MQW structure by electric

- fields," in *Extended Abstracts 18th (1986 Int.) Conf. Solid State Dev. Mater.*, Tokyo, Japan, pp. 595-598, 1986.
- [10] I. Suemune, T. Takeoka, M. Yamanishi, and Y. Lee, "Gain-switching characteristics and fast transient response of three-terminal size-effect modulation laser," *IEEE J. Quantum Electron.*, vol. QE-22, pp. 1900-1908, Sept. 1986.
- [11] T. Takeoka, M. Yamanishi, Y. Kan, and I. Suemune, "A 140 psec optical pulse generation by field-induced gain switching in a photo-excited quantum well laser," *Japan. J. Appl. Phys.*, vol. 26, pp. L117-L119, 1987.
- [12] T. H. Wood, C. A. Burrus, D. A. B. Miller, D. S. Chemla, T. C. Damen, A. C. Gossard, and W. Wiegmann, "High-speed optical modulation with GaAs/AlGaAs quantum wells in a p-i-n diode structure," *Appl. Phys. Lett.*, vol. 44, pp. 16-18, 1984.
- [13] —, "131 ps optical modulation in semiconductor multiple quantum wells (MQW's)," *IEEE J. Quantum Electron.*, vol. QE-21, pp. 117-118, Feb. 1985.
- [14] S. Tarucha, H. Iwamura, T. Saku, and H. Okamoto, "Waveguide-type optical modulator of GaAs quantum well double heterostructures using electric field effects on exciton absorption," *Japan. J. Appl. Phys.*, vol. 24, pp. L442-L444, 1985.
- [15] T. H. Wood, C. A. Burrus, R. S. Tucker, J. S. Weiner, D. A. B. Miller, D. S. Chemla, T. C. Damen, A. C. Gossard, and W. Wiegmann, "100 ps waveguide multiple quantum well (MQW) optical modulator with 10:1 on/off ratio," *Electron. Lett.*, vol. 21, pp. 693-694, 1985.
- [16] D. A. B. Miller, D. S. Chemla, T. C. Damen, A. C. Gossard, W. Wiegmann, T. H. Wood, and C. A. Burrus, "Novel hybrid optical bistable switch: The quantum well self-electro-optic effect device," *Appl. Phys. Lett.*, vol. 45, pp. 13-15, 1984.
- [17] D. A. B. Miller, D. S. Chemla, T. C. Damen, T. H. Wood, C. A. Burrus, A. C. Gossard, and W. Wiegmann, "The quantum well self-electrooptic effect device: Optoelectronic bistability and oscillation, and self-linearized modulation," *IEEE J. Quantum Electron.*, vol. QE-21, pp. 1462-1476, Sept. 1985.
- [18] S. Tarucha and H. Okamoto, "Voltage-controlled optical bistability associated with two-dimensional exciton in GaAs-AlGaAs multi quantum well lasers," *Appl. Phys. Lett.*, vol. 49, pp. 543-545, 1986.
- [19] H. Yamamoto, M. Asada, and Y. Suematsu, "Electric-field-induced refractive index variation in quantum-well structure," *Electron. Lett.*, vol. 21, pp. 579-580, 1985.
- [20] D. A. B. Miller, D. S. Chemla, T. C. Damen, A. C. Gossard, W. Wiegmann, T. H. Wood, and C. A. Burrus, "Band-edge electroabsorption in quantum well structures: The quantum-confined Stark effect," *Phys. Rev. Lett.*, vol. 53, pp. 2173-2176, 1984.
- [21] —, "Electric field dependence of optical absorption near the band gap of quantum-well structures," *Phys. Rev.*, vol. B32, pp. 1043-1060, 1985.
- [22] D. A. B. Miller, J. S. Weiner, and D. S. Chemla, "Electric-field dependence of linear optical properties in quantum well structures: Waveguide electroabsorption and sum rules," *IEEE J. Quantum Electron.*, vol. QE-22, pp. 1816-1830, Sept. 1986.
- [23] M. Erman, J. B. Theeten, P. Frijlink, S. Gaillard, Fan Jia Hia, and C. Alibert, "Electronic states and thickness of GaAs/GaAlAs quantum wells as measured by electroreflectance and spectroscopic ellipsometry," *J. Appl. Phys.*, vol. 56, pp. 3241-3249, 1984.
- [24] C. Alibert, S. Gaillard, J. A. Brum, G. Bastard, F. Frijlink, and M. Erman, "Measurements of electric-field-induced energy-level shifts in GaAs single-quantum wells using electroreflectance," *Solid State Commun.*, vol. 53, pp. 457-460, 1985.
- [25] H. Nagai, M. Yamanishi, Y. Kan, and I. Suemune, "Electroreflectance spectra and field-induced variation in refractive index of a GaAs/AlAs quantum well structure at room temperature," *Japan. J. Appl. Phys.*, vol. 25, pp. L640-L642, 1986; H. Nagai, Y. Kan, M. Yamanishi, I. Suemune, Y. Ide, and R. Lang, "Exciton-induced dispersion of electroreflectance in a GaAs/AlAs quantum well structure at room temperature," in *Extended Abstracts 18th (1986 Int.) Conf. Solid State Dev. Mater.*, Tokyo, Japan, pp. 591-594, 1986.
- [26] H. Nagai, M. Yamanishi, Y. Kan, and I. Suemune, "Field-induced modulations of refractive index and absorption coefficient in a GaAs/AlGaAs quantum well structure," *Electron. Lett.*, vol. 22, pp. 888-889, 1986.
- [27] Y. Kan, M. Yamanishi, H. Nagai, and I. Suemune, "Electro-optic effect in a GaAs/AlGaAs quantum well structure at room temperature," in *Proc. Int. Symp. GaAs, Related Compounds*, Las Vegas, NV, 1986.
- [28] M. Yamanishi and I. Suemune, "Comment on polarization dependent momentum matrix elements in quantum well lasers," *Japan. J. Appl. Phys.*, vol. 23, pp. L35-L36, 1984.
- [29] T. Hiroshima, "Electric field induced refractive index changes in GaAs-Al_xGa_{1-x}As quantum wells," *Appl. Phys. Lett.*, vol. 50, pp. 968-970, 1987.
- [30] B. O. Seraphin, *Semiconductors and Semimetals*. New York: Academic, 1972, vol. 9, ch. 1, pp. 8-13.
- [31] F. Koyama, and K. Iga, "Frequency chirping of external modulation and its reduction," *Electron. Lett.*, vol. 21, pp. 1065-1066, 1985.
- [32] I. D. Henning and J. V. Collins, "Measurements of the semiconductor laser linewidth broadening factor," *Electron. Lett.*, vol. 19, pp. 927-929, 1983.
- [33] T. H. Wood, R. W. Tkach, and A. R. Chraplyvy, "Observation of large quadratic electro-optic effect in GaAs/AlGaAs multiple quantum wells," *Appl. Phys. Lett.*, vol. 50, pp. 798-800, 1987.
- [34] S. Sakano, H. Inoue, H. Nakamura, T. Katsuyama, and H. Matsunaga, "InGaAsP/InP monolithic integrated circuit with laser and an optical switch," *Electron. Lett.*, vol. 22, pp. 594-596, 1986.
- [35] G. Bastard, E. E. Mendez, L. L. Chang, and L. Esaki, "Variational calculations on a quantum well in an electric field," *Phys. Rev. B*, vol. 28, pp. 3241-3245, 1983.
- [36] J. A. Brum and G. Bastard, "Electric-field-induced dissociation of excitons in semiconductor quantum wells," *Phys. Rev. B*, vol. 31, pp. 3893-3898, 1985.
- [37] T. Sakamoto, H. Funabashi, K. Ohta, T. Nakagawa, N. J. Kawai, and T. Kojima, "Phase-locked epitaxy using RHEED intensity oscillation," *Japan. J. Appl. Phys.*, vol. 23, pp. L657-L659, 1984.
- [38] Y. Horikoshi, M. Kawashima, and H. Yamaguchi, "Low-temperature growth GaAs and AlAs-GaAs quantum well layers by modified molecular beam epitaxy," *Japan. J. Appl. Phys.*, vol. 25, pp. L868-L870, 1986.
- [39] Y. Kan, M. Yamanishi, Y. Usami, and I. Suemune, "Switching of photoluminescence by pulsed electric field in GaAs/Al_{0.7}Ga_{0.3}As single quantum well structure," *IEEE J. Quantum Electron.*, vol. QE-22, pp. 1837-1844, Sept. 1986.
- [40] H. C. Casey and M. B. Panish, *Heterostructure Lasers, Part A*. New York: Academic, 1978, ch. 3.6, p. 146.
- [41] —, *Heterostructure Lasers, Part A*. New York: Academic, 1978, ch. 3.6, pp. 150-158.
- [42] R. C. Miller, D. A. Kleinman, and A. C. Gossard, "Energy-gap discontinuities and effective masses for GaAs-Al_xGa_{1-x}As quantum wells," *Phys. Rev.*, vol. B29, pp. 7085-7087, 1984.



Yasuo Kan was born in Ehime, Japan, on January 18, 1960. He received the B.E. and M.E. degrees from Hiroshima University, Higashihiroshima, Japan, in 1982 and 1984, respectively.

He joined the Department of Physical Electronics, Faculty of Engineering, Hiroshima University, Higashi-hiroshima-shi, Japan, in 1985 as a Research Associate and has been engaged in research on semiconductor lasers.

Mr. Kan is a member of the Japan Society of Applied Physics.



Hideo Nagai was born in Hiroshima, Japan, in 1962. He received the B.E. and M.E. degrees from Hiroshima University, Higashi-hiroshima-shi, Japan, in 1985 and 1987, respectively.

He joined the Matsushita Electric Industrial Co., Ltd., Osaka, Japan, in 1987.

Mr. Nagai is a member of the Japan Society of Applied Physics.



Masamichi Yamanishi (M'72) was born in Osaka, Japan, on January 31, 1941. He received the B.E., M.E., and Ph.D. degrees from the University of Osaka Prefecture, Osaka, Japan, in 1964, 1966 and 1971, respectively.

He joined the Department of Electrical Engineering, University of Osaka Prefecture, in 1966 as a Research Associate. In 1979, he was appointed Associate Professor in the Department of Physical Electronics, Hiroshima University, Higashi-hiroshima-shi, Japan. Since 1983, he has been a Professor, and is directing a research group on optoelectronics in the Department. In 1984, 1986, and 1987, he spent several months as a Visiting Professor at Purdue University, Lafayette, IN. He has been engaged in research on SAW acoustoelectric devices and acoustic DFB lasers. Currently, he is interested in research on semiconductor lasers, optical properties of quantum well structures and their device applications, and photoacoustic spectroscopy.

Dr. Yamanishi is a member of the Physical Society of Japan, the Japan Society of Applied Physics, and the Institute of Electronics and Communication Engineers of Japan.



Ikuo Suemune was born in Hyogo, Japan, on January 21, 1950. He received the B.E. degree from Hiroshima University, Higashi-hiroshima-shi, Japan, in 1972, and the M.E. and Ph.D. degrees from the Tokyo Institute of Technology, Tokyo, Japan, in 1974 and 1977, respectively.

He joined the Department of Physical Electronics, Hiroshima University, in 1977 as a Research Associate. Since 1983 he has been an Associate Professor. He has been engaged in research on SAW guides, microwave IMPATT oscillators, acoustical investigations of nonradiative recombinations in semiconductors and semiconductor lasers, epitaxial growth of II-VI compound semiconductor films such as ZnSe by MOCVD technique, two-dimensional and multiple-stripe lasers, and functional semiconductor lasers such as the electronic beam scannable and SEM laser.

Dr. Suemune is a member of the Japan Society of Applied Physics and the Institute of Electronics and Communication Engineers in Japan.